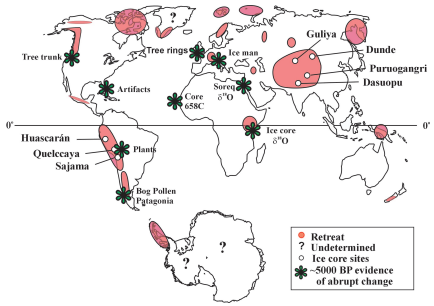

Fig. 1. The locations of ice cores and evidence for abrupt climate change ~5,000 yr ago discussed in the text are shown along with areas of large-scale ice retreat.

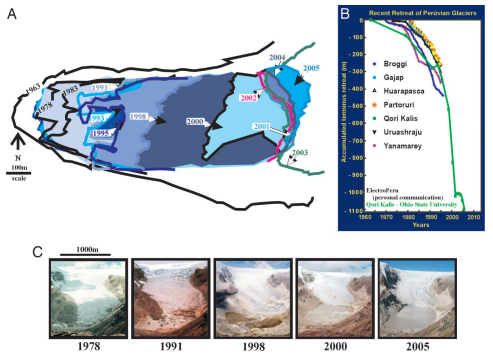

Fig. 2. Glacier retreat as documented in the Peruvian Andes. (*A*) Retreat of Qori Kalis from 1963 to 2005. (*B*) Retreat records for Qori Kalis and six other Andean glaciers. (*C*) The photos document the expansion of the proglacial lake from 1991 to 2005 as Qori Kalis retreated.

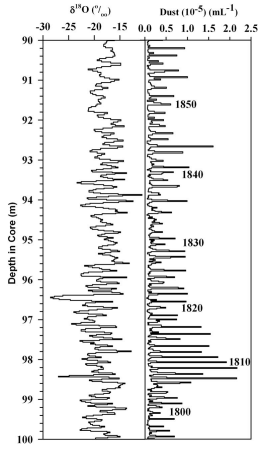

Fig. 3. The excellently preserved seasonal variations in $\delta^{18}O$ and insoluble dust, illustrated for the core section from 90 to 100 m depth, were used to date the 2003 Quelccaya ice core and reconstruct the annual accumulation history.

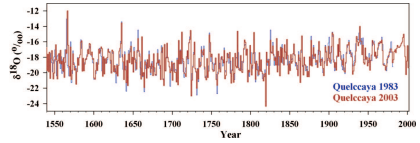

Fig. 4. The annual average $\delta^{18}O$ values for the 1983 Quelccaya core, measured on bottled water from samples cut and melted in the field, are compared with those for the 2003 Quelccaya core, which were returned frozen to Ohio State University, allowing freshly cut samples to be analyzed. Even after 20 yr of surface melting, the reproducibility over the last 460 yr is excellent. For data, see Data Set 1, which is published as supporting information on the PNAS web site.

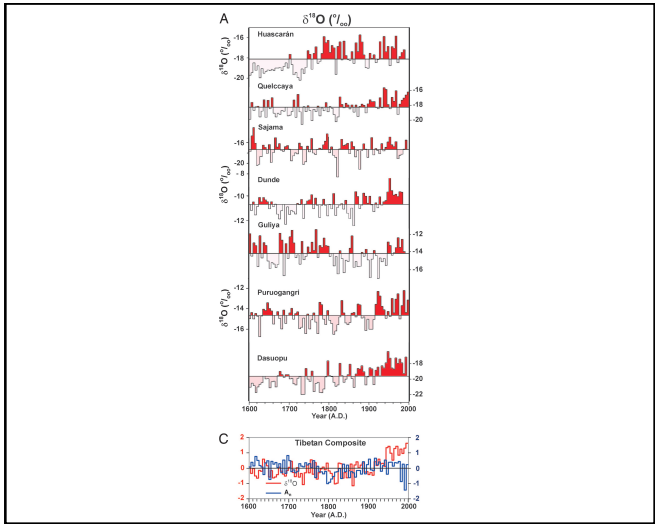

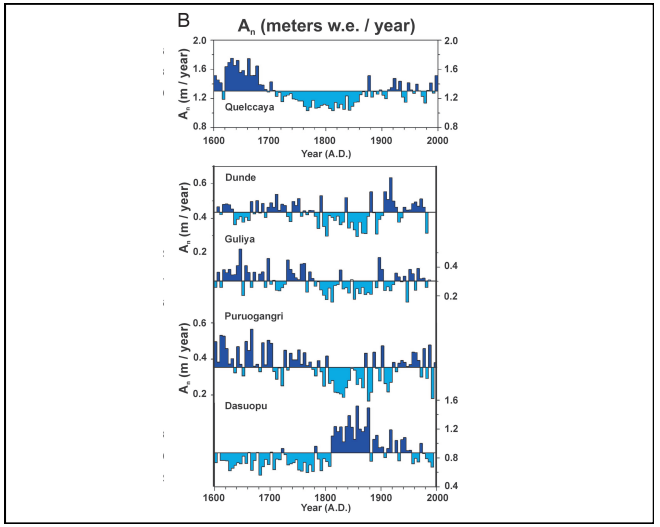

Kilimanjaro

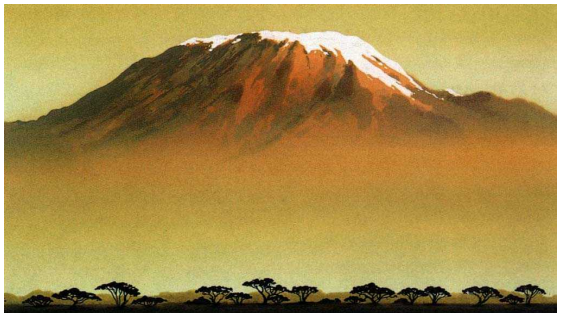

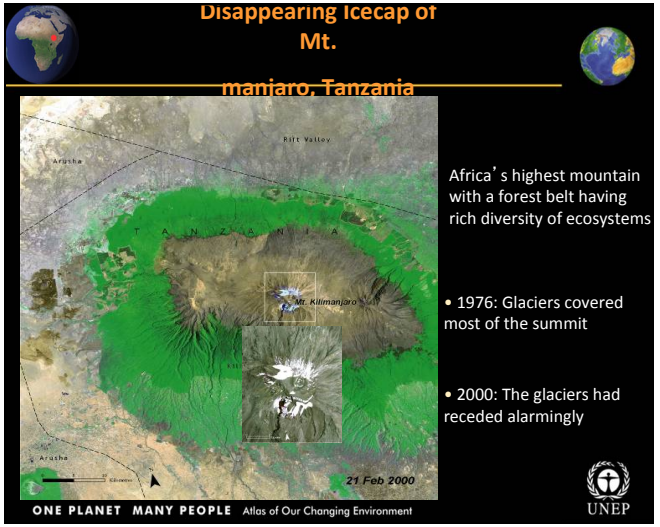

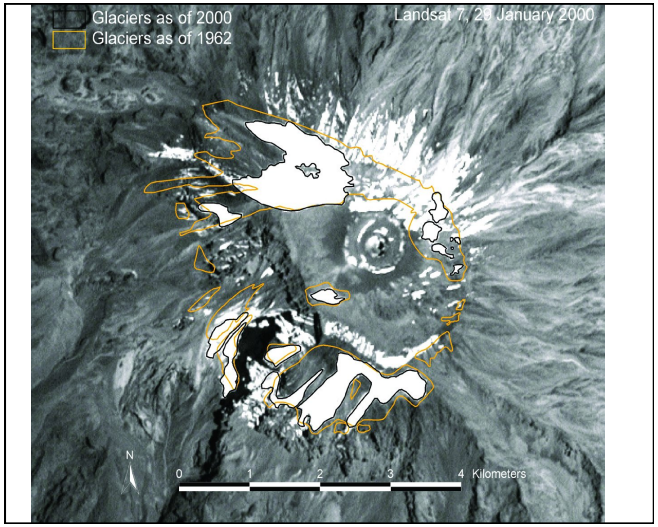

- Over the 20th century, the areal extent of Kilimanjaro's ice fields have decreased by ~80%
- If current climatolgical conditions persist, the remaining ice fields are likely to disappear between 2015 and 2020

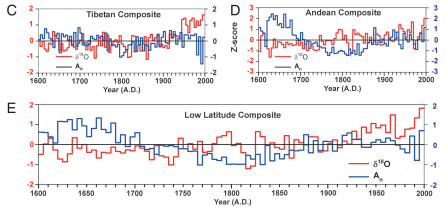

Fig. 5. Climate reconstructions over the last four centuries. The 5-yr averages of $\delta^{18}O$ (*A*) and accumulation (*B*) for seven and five low-latitude ice cores, respectively, were reconstructed back to A.D. 1600. Accumulation is given in meters of water equivalent (w.e.) per yr. Annual layers (and hence A_n) were not reconstructed for Huascarán and Sajama as discussed in the text. Composite $\delta^{18}O$ and A_n records for the TP (*C*) and Andean (*D*) cores were combined to produce low-latitude composite $\delta^{18}O$ and A_n histories (*E*) for the last 400 yr. The composite records are shown as *Z*-scores. Data are provided in Data Set 2, which is published as supporting information on the PNAS web site.

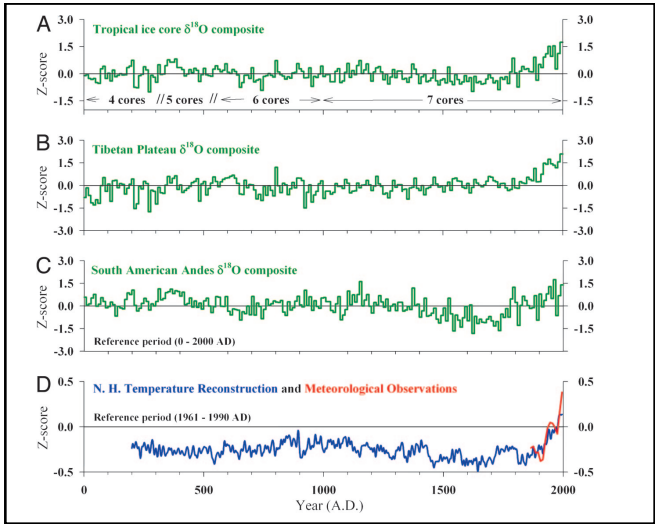

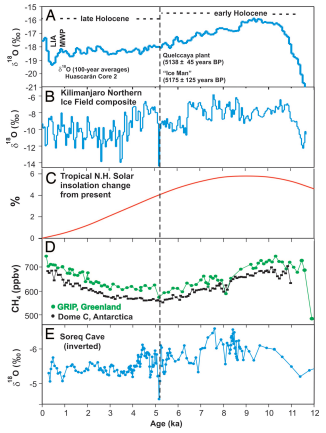

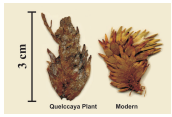

Fig. 8. Holocene tropical climate variability. Holocene $\delta^{18}O$ ice-core records recovered from Huascarán (23) (*A*) and Kilimanjaro (8) (*B*) along with tropical Northern Hemisphere (N.H.) insolation change from the present (33) (*C*), methane records from Greenland (37) and Antarctica (38) (*D*), and the Soreq Cave $\delta^{18}O$ record (43) (*E*). GRIP, Greenland Ice Core Project; ppbv, parts per billion by volume.

A review of the South American monsoon history as recorded in stable isotopic proxies over the past two millennia

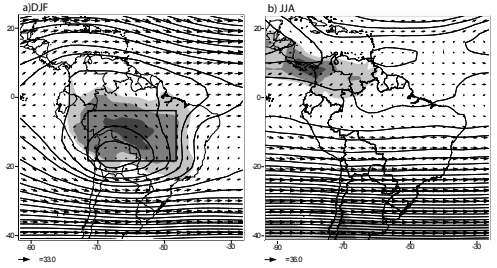

Fig. 1. Long-term mean 200 hPa wind and geopotential height and outgoing long-wave radiation based on NCEP/NCAR reanalysis and NOAA-OLR data for **(a)** austral summer (December–February, DJF) and **(b)** winter (June–August, JJA). Contour interval is 25 gpm, 10 gpm above 12 400 and 5 gpm above 12 430. Light, medium, and dark shades indicate OLR values less than 225, 210, and 195 W m^{-2}. Black rectangle in **(a)** denotes region of strongest convective activity during DJF used to create monsoon index *M*.

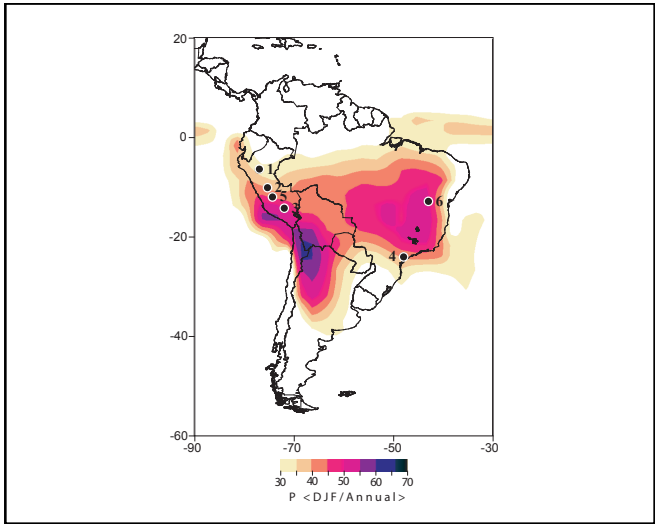
20
0
-20
-40
-60
-90
-70
-50
-30
1
2
3
4
5
6
30
40
50
60
70
P <DJF/Annual>

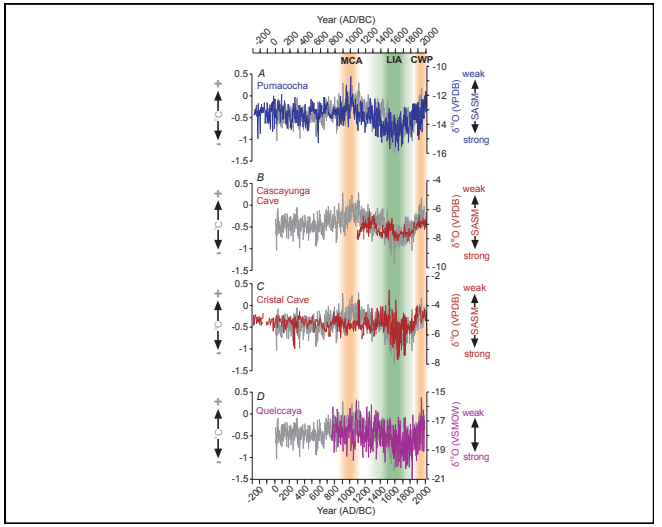
Year (AD/BC)
MCA
LIA
CWP
A
Pumacocha
B
Cascayunga Cave
C
Cristal Cave
D
Quelccaya
δ18O (VPDB)
δ18O (VSMOW)
weak
strong
SASM
Year (AD/BC)

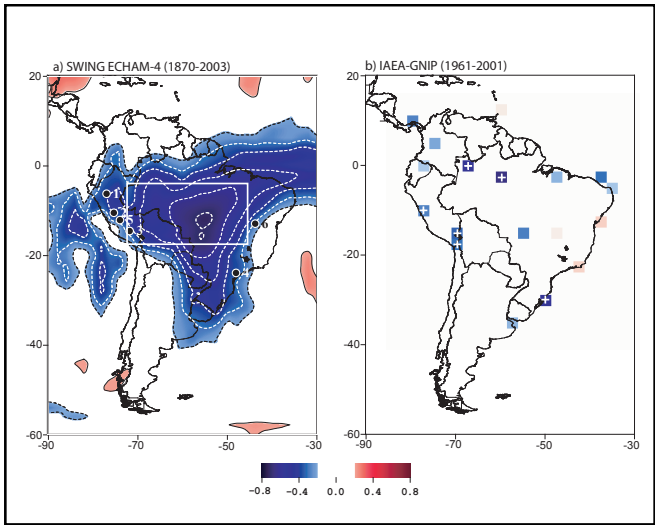
a) SWING ECHAM-4 (1870-2003)
b) IAEA-GNIP (1961-2001)
20
0
-20
-40
-60
-90
-70
-50
-30
−0.8
−0.4
0.0
0.4
0.8